Failure Mechanisms of Polymer Interfaces Reinforced with Block Copolymers†

Costantino Creton‡ and Edward J. Kramer*

Department of Materials Science and Engineering and the Materials Science Center, Cornell University, Ithaca, New York 14853

Chung-Yuen Hui

Department of Theoretical and Applied Mechanics and the Materials Science Center, Cornell University, Ithaca, New York 14853

Hugh R. Brown‡

Engineering Program, The Faculties, Australian National University, GPO Box 4, Canberra, ACT 2601, Australia

Received November 30, 1991; Revised Manuscript Received March 4, 1992

ABSTRACT: The fracture toughness (characterized by the critical energy release rate G_c) of interfaces between polystyrene (PS) and poly(2-vinylpyridine) (PVP) reinforced with poly(styrene-*b*-2-vinylpyridine) was measured with a double cantilever beam test geometry. The effect of the PVP block degree of polymerization (N_{PVP}) and the areal density of block copolymer chains at the interface (Σ) on the measured G_c and on the fracture mechanisms was investigated quantitatively. The PS degree of polymerization (N_{PS}) was kept >280, while N_{PVP} was varied between 45 and 870. For N_{PVP} below 200 the interfaces showed only a small increase in G_c with increasing Σ and failed by pull-out of the short PVP chain. In this regime G_c increases linearly with Σ and scales roughly with N_{PVP}^2, in reasonable agreement with a recently proposed model of failure by chain pull-out.[1] If N_{PVP} was increased well above 200, corresponding roughly to the average molecular weight between entanglements for the PVP, two separate fracture mechanisms could be distinguished. At low values of Σ, G_c increased only slowly with Σ and the interfaces failed by scission of the copolymer chains near the joint between the two blocks. At higher values of Σ, the interfaces fractured by first forming a stable craze ahead of the propagating crack tip, giving rise to much higher values of the measured fracture toughness. In this regime, G_c scaled with Σ_{eff}^2, an areal density of chains with at least one "effective" entanglement, in very good agreement with a model recently proposed by Brown[2] for failure by craze fibril breakdown.

1. Introduction

Binary blends of polymers are generally immiscible and form a phase-separated mixture. The necessary conditions to obtain good mechanical properties from the blend are a fine dispersion of the second-phase particles and a good adhesion between the matrix and the particle to avoid debonding at low levels of stress. These conditions are not met for most polymer systems, and one of the approaches to improve the mechanical properties of the blend is to add a properly chosen block copolymer.

Experimentally, it has been known for some time that A–B diblock copolymers added to an immiscible blend of A and B polymers decrease the phase size of the second-phase particles and generally improve the overall mechanical properties.[3–6] This effect has been attributed to the tendency of the block copolymer to segregate at the interface between the two phases for thermodynamic reasons, causing a decrease of the interfacial tension as well as an improvement of the adhesion between the particle and the matrix. The block copolymer acts mechanically by entangling on both sides of the interface with the respective homopolymers as shown schematically in Figure 1, forming effective "stitches" between the two phases. Although this basic principle by which the block copolymer acts at the interface is known, the detailed micromechanical processes by which the presence of the block copolymer leads to a reinforcement and the influence of such basic parameters as the amount of block copolymer present at the interface or the molecular weight of its respective blocks are still far from being thoroughly understood. In a previous study[7] we investigated qualitatively the effect of the block copolymer addition on the strength of the interface. Although an addition of block copolymer decreased the interfacial tension in every case, only those block copolymers with a block molecular weight greater than the average molecular weight between entanglements M_e had an appreciable mechanical reinforcement effect. The TEM technique employed in that study allowed us to investigate the deformation behavior of a realistic blend through the statistical observation of failed particle–matrix interfaces; however, no information was available on the amount of block copolymer actually present at the interface or on the maximum stress that could be sustained by the interface before failure.

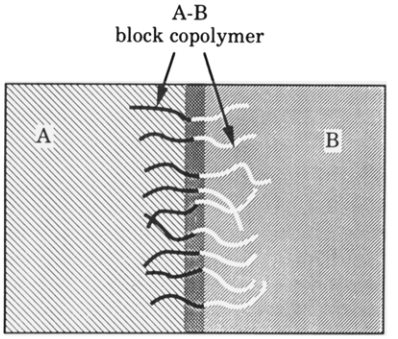

Figure 1. Schematic of a layer of A–B block copolymer chains segregated at the interface between A and B homopolymers.

To obtain such information, a test must be devised where a single interface is tested and a detailed knowledge of the

† Report No. 7278 of the Materials Science Center.
‡ Present address: IBM Almaden Research Center, 650 Harry Road, San Jose, CA 95120.

0024-9297/92/2225-3075$03.00/0

Table I
Degrees of Polymerization and Polydispersity of the Block Copolymers

N		
dPS block	PVP block	$\bar{M}_w/\bar{M}_n$
625	49	1.02
280	52	1.08
680	100	1.04
1300	173	1.07
420	270	1.04
510	540	1.07
800	870	1.1

amount of block copolymer present is available. Brown and co-workers have adapted a double cantilever beam (DCB) test geometry to the case of polymer interfaces reinforced by block copolymers. They investigated interfaces between PS and PMMA and between PMMA and PPO which were reinforced by an addition of PS–PMMA block copolymers,[8] and their study focused on a regime where the toughness of the interface is molecular weight independent, i.e., in the case where the block molecular weights are far above the entanglement molecular weight of the respective homopolymers and where one expects failure by chain scission at the interface.

Very little has been done in the molecular weight dependent regime of the fracture toughness, i.e., where significant pull-out or disentanglement of the chains occurs during the interfacial failure. The purpose of this study is to investigate quantitatively the dependence of the fracture toughness of the interface on the areal density and molecular weight of the added block copolymer, thereby gaining a molecular understanding of the different failure mechanisms.

The experimental system we have chosen for this investigation is the immiscible pair of homopolymers polystyrene (PS) and poly(2-vinylpyridine) (PVP). Both polymers have approximately the same glass transition temperature and, because of their similar molecular structure, have a similar average molecular weight between entanglements, as determined by measurements of the shear modulus in the rubbery plateau regime. Both polymers deform plastically by crazing in preference to shear deformation. It should be noted however that the elastic modulus and the crazing stress of the two materials are somewhat different, and these differences will have important implications in the interpretation of our experimental results of the fracture toughness of interfaces between the two polymers. The very strong immiscibility of PS and PVP is responsible for very sharp interfaces with very little chain interpenetration in the absence of block copolymer. Such "bare" interfaces are very weak and justify our implicit assumption that the block copolymer chains at the interface are the sole cause of the measured mechanical strength.

2. Experimental Methods

2.1. Materials. Diblock copolymers of PS and PVP with nearly monodisperse block lengths were prepared by anionic polymerization using a cumylpotassium initiator. The polymerization was carried out at −55 °C in tetrahydrofuran, and the characteristics of the resulting diblock copolymers are shown in Table I. All block copolymers were prepared with a deuterated polystyrene block (dPS) in order to be used as markers in a forward recoil spectrometry (FRES) experiment. The diblock copolymers will be designated by the polymerization indices of their two blocks so that, for example, the block copolymer consisting of a dPS block with a degree of polymerization 390 and a PVP block with degree of polymerization 150 will be designated as 390–150. The homopolymer PS (commercial grade, $\bar{M}_n$ = 250 000) was purchased from Aldrich Chemical Co., and the homopolymer PVP (commercial grade, $\bar{M}_n$ = 200 000) was purchased from Polysciences.

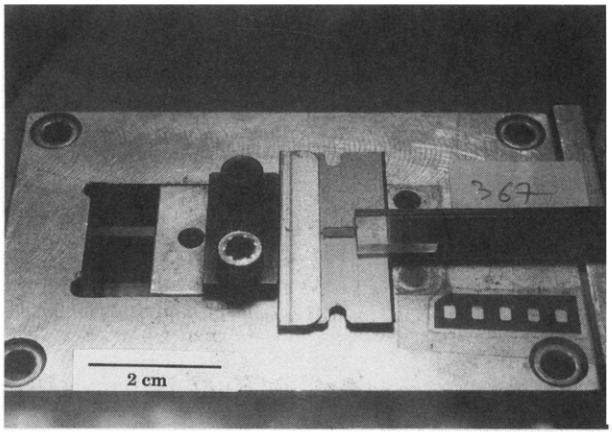

Figure 2. Experimental setup for the fracture toughness test. Note that the crack tip is clearly visible through the transparent polystyrene top layer.

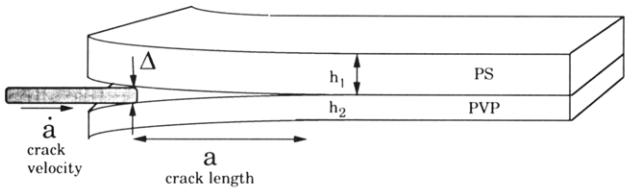

Figure 3. Geometrical parameters of the asymmetric double cantilever beam test sample used for the fracture toughness test.

2.2. Fracture Toughness Test. The PS and the PVP were compression molded into sheets 7.5 cm × 5 cm with respective thicknesses of 2.3 and 1.7 mm. A thin (10–600 Å) film of dPS–PVP block copolymer was then spun cast on the PVP sheet from a toluene solution. After a drying step of 1 h at 80 °C under vacuum, the PS sheet was placed on top of the PVP sheet and the sample was annealed for 2 h at 160 °C in air under slight pressure to ensure contact between the two sides. Each sandwich was then cut into strips 8.5 mm × 50 mm which were dried at 80 °C under vacuum for 8 h prior to mechanical testing. The mechanical test was performed by inserting a wedge, namely, a single-edged razor blade, at the interface as shown in Figure 2 and pushing it in at a constant velocity of 3×10^{-6} m/s using a servomotor. The length of the crack ahead of the blade was measured by taking photographs of the advancing crack at regular intervals with a camera connected with an intervalometer. In this way at least 20 values of the fracture toughness could be obtained for each specimen and a mean and a variance could be computed. The validity of such a test has been demonstrated by Brown[9] in the case of interfaces between PS and PMMA where the results of the DCB test at constant opening displacement were compared with results obtained at constant load where the load on the two faces of the sandwich sample was applied by an Instron tensile testing machine.

The chosen test geometry was an asymmetric double cantilever beam as shown in Figure 3. The reason for using this asymmetric test geometry lies in the different elastic moduli of the two materials as well as their different crazing stresses. In a symmetric configuration, the double cantilever beam loading geometry would create a K_{II} component in the stress intensity factor at the crack tip causing the crack to swerve toward the more compliant material. If the more compliant material also has a lower crazing stress, small crazes will grow at an angle from the plane of the main crack. These small crazes can contribute significantly to the measured fracture toughness.[9] To avoid such an effect it is desirable to make the sample configuration asymmetric; i.e., the plate made of the stiffer material is made thinner to keep the crack at the interface. A more detailed discussion on crack propagation at bimaterial interfaces can be found in ref 10. A plot of the measured fracture toughness G_c in the case of PS–PVP interfaces without any block copolymer is shown as a

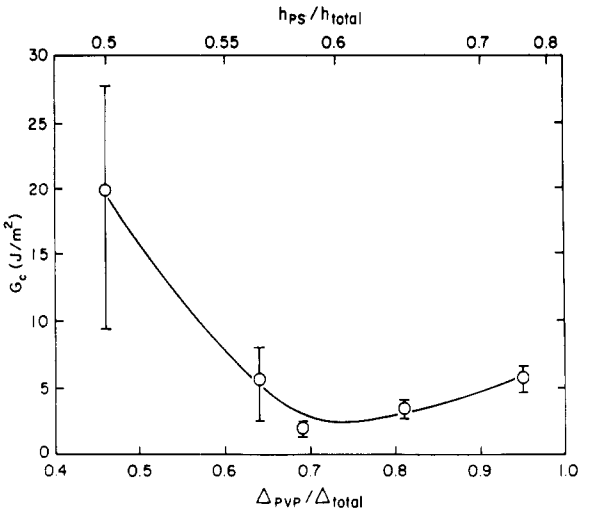

Figure 4. Fracture toughness of the interface, G_c as a function of the degree of asymmetry. The full line is drawn to guide the eye.

function of the degree of asymmetry in Figure 4, where the degree of asymmetry is characterized by the ratio of the opening displacement of the PVP half-sample relative to the total opening displacement ($\Delta_{PVP}/\Delta_{total}$). The partial opening displacement Δ_{PVP} is given by

$$\Delta_{PVP} = \frac{\Delta_{total} E_{PS} h_{PS}^3 C_{PVP}^3}{E_{PVP} h_{PVP}^3 C_{PS}^3 + E_{PS} h_{PS}^3 C_{PVP}^3} \quad (1)$$

with $C_{PS} = 1 + 0.64h_1/a$ and $C_{PVP} = 1 + 0.64h_{PVP}/a$. h_{PS} and h_{PVP} are the respective thicknesses of the beams, Δ_{total} is the thickness of the wedge, a is the crack length, and E_{PS} and E_{PVP} are the elastic moduli. This expression is obtained from a model of a cantilever beam on an elastic foundation explained in more detail in section 3.

It is clear from the data that significant differences in the measured G_c can occur if the crack is allowed to deviate toward the PS. When the difference in the crazing stresses of the two materials is relatively small, one might expect a deviation of the crack into the other material if the sample is made too asymmetric. For all our experiments we chose the geometry corresponding to the lowest measured value of G_c ($\Delta_{PVP}/\Delta_{total} = 0.65$) assuming that such a configuration would minimize the mode II component of the stress intensity factor and prevent therefore the formation of crazes in the more compliant bulk material. However, because, strictly speaking, a pure mode I crack propagation at an interface between dissimilar materials can never be achieved, we chose, in this paper, to label the measured fracture toughness G_c rather than G_{Ic}.

A very important experimental asset of this study is our capability to measure the areal density of block copolymer at the interface by using three surface analysis techniques, namely, forward recoil spectrometry (FRES), Rutherford backscattering spectrometry (RBS), and X-ray photoelectron spectroscopy (XPS). The areal density of deuterium atoms N_D present on each of the two fracture surfaces can be obtained by FRES.

The areal density of chains Σ is then calculated by dividing N_D by the number of deuterium atoms per chain. This method however does not give any indication about the location of the PVP block after fracture. Although it is impossible to detect any PVP block on the PVP side because the PVP block and the PVP homopolymer are chemically identical, several methods can be used to detect PVP on the PS side. In one method the PS side of the sample is exposed to methyl iodide vapor which reacts selectively with PVP, quaternizing it. The sample is then analyzed with RBS and the amount of iodine detected is directly proportional to the amount of PVP present on the fracture surface. A second method which can be used is the direct analysis of the PS fracture surface with XPS. The ratio of nitrogen to carbon near the surface (within 50 Å) can be measured, and an estimate of the amount of PVP at the surface can be obtained from it.

2.3. Optical Interference Microscopy. Due to the transparent nature of the polystyrene and our specific testing geometry, it was possible to observe interference fringes from light reflected on both sides of the crack or the craze. This experiment was performed with a reflected light Olympus microscope using a monochromatic beam with a 550-nm wavelength. The wedge was inserted at the interface and the sample was then observed under the microscope until no further advance of the crack was visible, at which point a photograph was taken effectively simulating a fracture test at a very slow crack velocity. Such an experimental technique, pioneered by the work of Bessonov and Kuvshinskii[11] and by Kambour,[12] provides a very elegant way to confirm the presence or the absence of a wide craze ahead of the crack tip as the pattern of the interference fringes is markedly different for the two cases.

3. Data Analysis

The critical crack extension force G_c can be obtained by assuming that all the elastic energy released upon fracture is dissipated in a region relatively small compared with the specimen dimensions. Most of this energy is absorbed by the plastic deformation taking place at the crack tip. The most simple approximation for the released elastic energy is to consider that the only contribution comes from the bending of the two beams and no energy is stored ahead of the crack tip. In this case G_c is given from simple beam theory by[13]

$$G_c = \frac{3\Delta^2 E_1 h_1^3 E_2 h_2^3}{8a^4[E_1 h_1^3 + E_2 h_2^3]} \quad (2)$$

where h_1, h_2, Δ, E_1, E_2, and a are as defined for eq 1 and where the subscripts 1 and 2 stand for PS and PVP. This relation is a good approximation as long as the crack is long relative to the thickness of the beams but overestimates G_c for the shorter crack lengths typical of stronger interfaces. A better description of the experimental data is given by a model of a cantilever beam on an elastic foundation derived by Kanninen.[14] In this model the beam is free in the fractured part of the sample and supported by an elastic foundation ahead of the crack tip. Admittedly, the foundation modulus is chosen rather arbitrarily; however, such a model seems to fit our experimental data better and the extracted values of fracture toughness are independent of the opening displacement as required. Although still an approximation, this method is the best available at this point and will be used in the following sections to extract G_c. A complete finite element analysis of the stress field in the double cantilever beam geometry is being presently developed and will be used in the future.

With the beam on an elastic foundation approximation, G_c is given by

$$G_c = \frac{3\Delta^2 E_1 h_1^3 E_2 h_2^3}{8a^4}\left[\frac{E_1 h_1^3 C_2^2 + E_2 h_2^3 C_1^2}{[E_1 h_1^3 C_2^3 + E_2 h_2^3 C_1^3]^2}\right] \quad (3)$$

with $C_1 = 1 + 0.64h_1/a$ and $C_2 = 1 + 0.64h_2/a$.

4. Results

4.1. Bulk Material Properties. To carry out the analysis of our results on interfaces, a certain number of material properties of the two bulk materials, PS and PVP, need to be known. The average molecular weight between entanglements was determined by the measurement of the elastic modulus in the rubbery plateau regime,[15] while the Poisson's modulus ν was determined by a measurement of the velocity of a transverse and longitudinal elastic wave at high frequency (1 MHz). The crazing stress and the elastic constants were also measured for PMMA to compare our results with the results obtained by Brown[8]

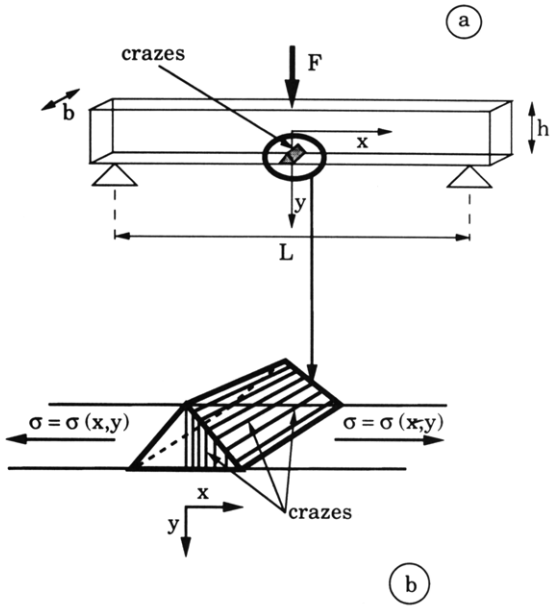

Figure 5. Experimental geometry for the three-point bending test used to determine the crazing stress and the elastic modulus of the bulk materials.

on interfaces between PMMA and PPO reinforced with PS–PMMA block copolymers.

Because both the crazing stress and the elastic modulus are strain rate dependent, one should be careful to measure these properties at a strain rate closely matching the strain rate in the double cantilever beam experiment. Our first step is to measure the crazing stress at a rate that is typical of our cantilever beam test. As crazes grow in width by pulling fresh material in the crazed zone, the best way to characterize the strain rate of a single craze is the widening velocity, generally called the drawing rate ($\dot{\delta}$). Using a crack velocity of 0.003 mm/s typical of our cantilever beam experiments on interfaces and the shape of the craze obtained from the analysis of Figure 14, $\dot{\delta}$ is estimated at 60 nm/s, where the relation

$$\dot{\delta} = \frac{d\delta}{dx}\dot{a} \tag{4}$$

has been used. The selected experimental technique to measure the crazing stress at a comparable widening velocity was a three-point bending test as shown in Figure 5.

In such a geometry the tensile stress in the bottom half of the sample is given by

$$\sigma_{xx} = \frac{Fy(L/2 - x)}{2I} \tag{5}$$

where x and y are coordinates relative to the center of the sample as defined in Figure 5a, F is the applied force, I is the moment of inertia of the beam, and L is the distance between the two supports. From the observation of the fracture surfaces as shown schematically in Figure 5b, it is possible to determine how far from the point of maximum tensile stress (defined as $x = 0$ and $y = h/2$ with our coordinate system) the crazes have extended and obtain a value of the crazing stress. A measurement of the number of crazes per unit length in the x direction allows us to estimate the widening velocity of a craze $\dot{\delta}$ for a specific macroscopic loading rate. Typically, a crosshead speed of 20 μm/s gives a strain rate of $\sim 1.5 \times 10^{-3}$ s^{-1} at the bottom of the beam, and with a craze density of $\sim$25 crazes/mm, we obtain $\dot{\delta} \sim 50$ nm/s, which is reasonably close to the value estimated for the double cantilever beam test.

Table II
Mechanical Properties of the Bulk Polymers

	E^a (MPa)	ν^b	N_e	$\sigma_d{}^c$ (MPa)
PS	3000	0.341	173[d]	55 ± 5
PVP	3500	0.325	255[e]	75 ± 5
PMMA	3300	0.325	90[f]	100 ● 10

[a] E is measured at a strain rate of $\dot{\epsilon} = 1 \times 10^{-6}$ s^{-1}. [b] ν is measured with an ultrasonic technique. [c] σ_d is measured at a craze widening velocity of $\sim$60 nm/s. [d] Onogi, S.; Masuda, T.; Kitagawa, K. *Macromolecules* **1970**, *2*, 109. [e] Jerry Seitz, Dow Chemical Co.; from a measurement of the shear modulus in the rubbery plateau regime. [f] Masuda, T.; Kitagawa, K.; Onogi, S. *Polym. J.* **1970**, *1*, 418.

For the tensile modulus, the strain rate at the bottom of the PS beam in our double cantilever beam experiment can be calculated from simple beam theory:

$$\dot{\epsilon} = 0.75\frac{\Delta h \dot{a}}{a^3} \tag{6}$$

where Δ is the opening displacement imposed by the razor blade, h is the beam thickness, a is the crack length, and $\dot{a}$ is the crack velocity. To estimate $\dot{\epsilon}$ we considered the strain distribution in the direction of crack propagation (on the side of the sample experiencing the maximum tensile stress) and used the relation

$$\dot{\epsilon} = \left(\frac{d\epsilon}{dx}\right)\left(\frac{dx}{dt}\right) \tag{7}$$

where x is the distance along the beam in the direction of crack propagation. With values typical of our experiment we find $\dot{\epsilon} \sim 10^{-7}$–$10^{-5}$ s^{-1}, and, consequently, the moduli have been measured with the three-point bending geometry with a deformation rate of $\dot{\epsilon} = 10^{-5}$ s^{-1}.

As evidenced by Table II, the values of the crazing stress measured by our technique appear to be higher than those usually found in the literature. In particular, Berger,[16] using a tensile test of a thin film, found $\sigma_d = 35$ MPa for PS. His experiment however was performed at a rate of $\dot{\delta} = 1$ nm/s, which is much lower than the drawing rate used in our test. This discrepancy, due to the different drawing rates, emphasizes the necessity to use appropriate values of σ_d and E to obtain results that are quantitatively correct.

It is important to note that PVP has a higher modulus and a higher crazing stress than PS. This asymmetry, although not very large, will significantly alter the fracture micromechanisms at the interface.

4.2. Fracture Toughness of the Interface. The measured values of G_c as well as the fracture mechanisms at the interface are dependent on both the areal density Σ of block copolymer chains at the interface and the respective degrees of polymerization of the blocks, N_{PS} and N_{PVP}. In our previous study,[7] it was found that the load-bearing capacity of the interface underwent a transition when N_{PVP} went from below to above the average degree of polymerization between entanglements of PVP (N_{ePVP}), and it is therefore interesting to examine the two cases separately.

To illustrate the sub-N_e case, plots of G_c vs Σ are shown in Figure 6 for several block copolymers. It should be pointed out at this stage that each data point is the average of roughly 20 measurements and the error bars represent one standard deviation to give an idea of the scattering in the data. This type of mechanical experiment typically results in a large scattering of the data points because of the difficulty to obtain exactly reproducible samples. In particular, small local departures from planarity of the interface can result in large changes in G_c. It is particularly

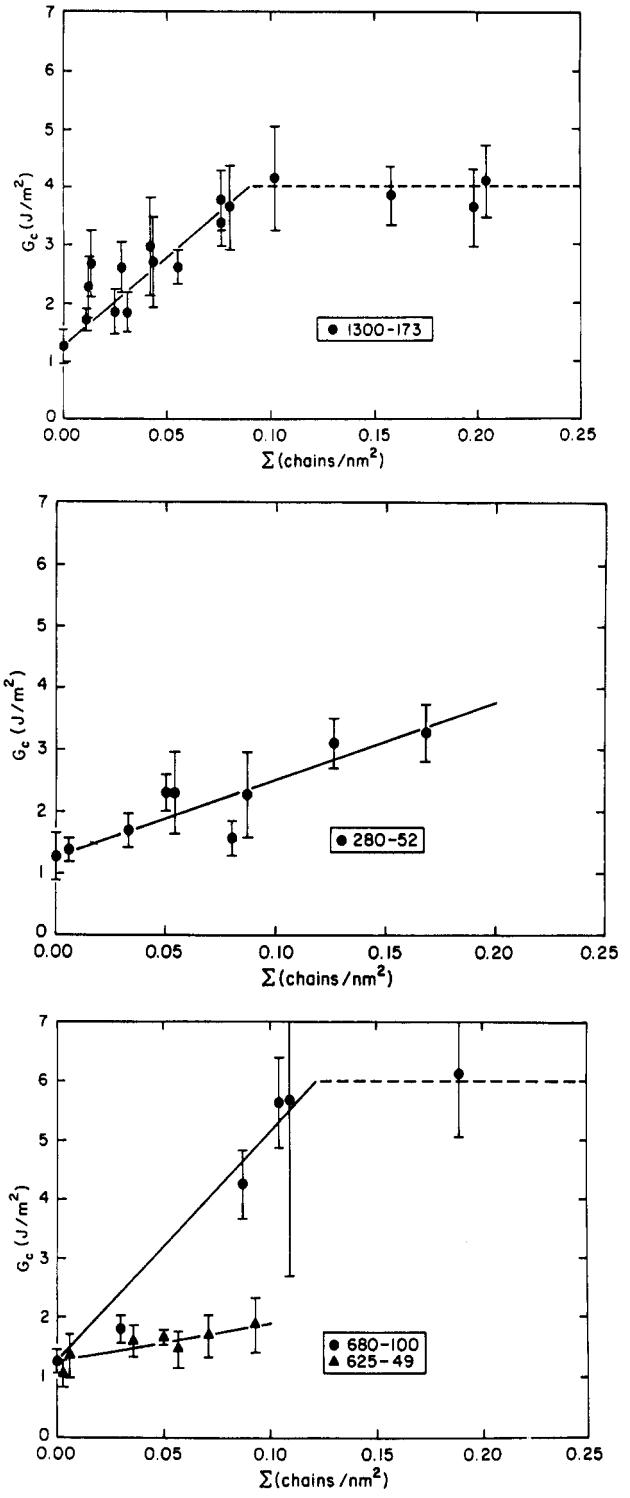

Figure 6. Fracture toughness G_c of interfaces reinforced with copolymers with a short PVP block: (a) 1300–173; (b) 280–52; (c) 680–100 and 625–49. The full lines are the best linear fit to the data in the regime below saturation. The slope of this fit gives a value of G_c/Σ.

important therefore to have a statistically significant number of measurements.

Figures 6a and 6b show the case of the 1300–173 and 280–52 block copolymers, respectively, while two copolymers having nearly the same N_{PS} but a different N_{PVP} are directly compared in Figure 6c.

In all cases, the measured fracture toughness increases linearly with Σ and then levels off at a constant value. For the 1300–173 copolymer, the areal density at which this leveling off occurs corresponds fairly well to the equilibrium areal density of block copolymer present at the interface which was obtained from a separate thermodynamic study on the same system.[17]

As the degree of polymerization of the PVP block is below N_{ePVP}, no effective entanglement should be formed between the PVP homopolymer and the PVP block of the copolymer, so that weak interfaces and low values of G_c are expected. For all block copolymers with N_{PVP} below N_{ePVP}, the maximum measured G_c was of the order of 5–10 J/m^2, which, although representing up to a sixfold increase relative to the toughness of a bare PS–PVP interface (~1.5 J/m^2), is still very low if it is compared with a value of ~500 J/m^2 characteristic of pure PS.

These results for copolymers with short PVP blocks are to be contrasted with those for copolymers with longer PVP blocks. When N_{PVP} is increased to N_{ePVP} and above, there should be effective entanglements between the block copolymer and the homopolymer chains so that a significant increase in G_c is expected. This expectation is borne out by our results. Three plots of G_c vs Σ for the "long PVP block" case are shown in Figure 7 for the 420–270, the 510–540, and the 800–870 copolymers where data from the 1300–173 copolymer are plotted in the same figure to allow an easy comparison. As for the "short PVP block" case, G_c increases monotonically with Σ and then levels off. The absolute values of the measured fracture toughness are now much higher however, upward to 100 J/m^2 for the 800–870 copolymer. As a first approximation, the best parameter to characterize the effectiveness of the reinforcement is the slope of the curve of G_c vs Σ measured in the regime below where the leveling off of G_c occurs. This parameter G_c/Σ effectively represents the energy per chain necessary to fracture the interface and is plotted in Figure 8 vs N_{PVP} for all the block copolymers investigated in this study. It is apparent from the data that G_c/Σ increases dramatically when $N_{PVP} > N_{ePVP}$, consistent with the results presented in ref 7 indicating that the necessary condition for an appreciable reinforcement was to have at least one entanglement on each side of the interface.

Although the main measurement characterizing the reinforcement effect of the block copolymer is the magnitude of G_c, the analysis and the observation of the fracture surfaces as well as the observation of the crack tip by optical interference microscopy provide further insight into the fracture mechanisms. The results of these experiments are best presented separately for the two cases of $N_{PVP} < N_{ePVP}$ and $N_{PVP} > N_{ePVP}$.

4.3. Short PVP Block (N_{PVP} below N_{ePVP}). As no effective entanglements are formed between the PVP block and the PVP homopolymer, it is reasonable to assume that the shorter PVP chains are being pulled out during the fracture process. A confirmation of this pull-out failure mechanism can be obtained from the surface analysis techniques.

All fracture surfaces of the samples tested mechanically were analyzed with FRES as described in section 2.2 and deuterium was found almost exclusively on the PS side (more than 95% in all cases), indicating that the dPS block stays anchored to the PS side during fracture. To illustrate this result, plots of the FRES spectrum of both fracture surfaces of a sample reinforced with a 1300–173 copolymer are shown in Figure 9. The plots show clearly that nearly all the dPS block remains on the PS side of the interface after fracture. The background away from the interface in the spectrum of the PS side is due to the block copolymer chains diffusing away from the interface. When the critical micelle concentration is of the order of a few percent, a nonnegligible amount of block copolymer will diffuse in the bulk polymer (in this case the PS) during the annealing phase so that the actual amount of block copolymer present

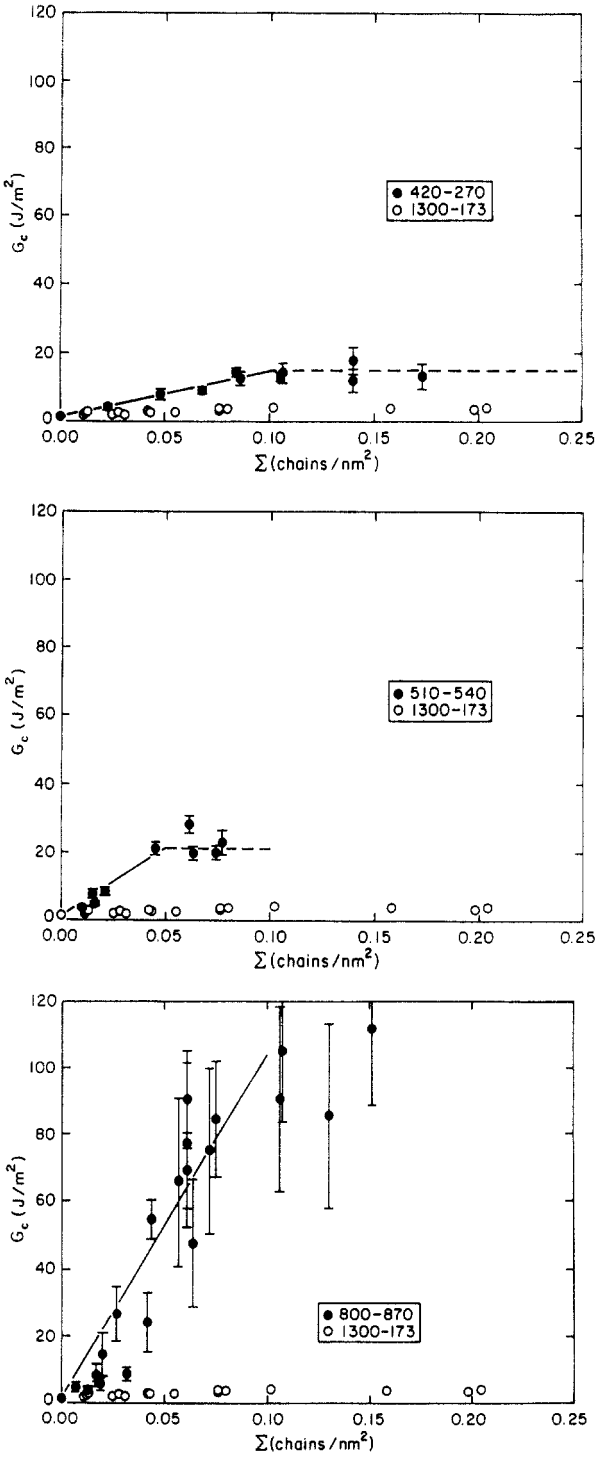

Figure 7. Fracture toughness G_c of interfaces reinforced with block copolymers with a long PVP block: (a) 420–270; (b) 510–540; (c) 800–870. The full line is the best linear fit used to extract a value of G_c/Σ.

at the interface at the moment of fracture will be lower than the nominal amount. This fact stresses the need for a technique such as FRES which allows the detection of the block copolymer after fracture.

It should also be pointed out that, as opposed to experiments on interfacial segregation where the block copolymer interfacial excess is the relevant quantity, the total amount of chains at the interface, as shown in the shaded area in Figure 9, is the quantity used here to obtain the areal density of chains Σ.

The location of the PVP block has been investigated with RBS and XPS. An RBS spectrum of the surface of the PS side previously stained with methyl iodide is shown

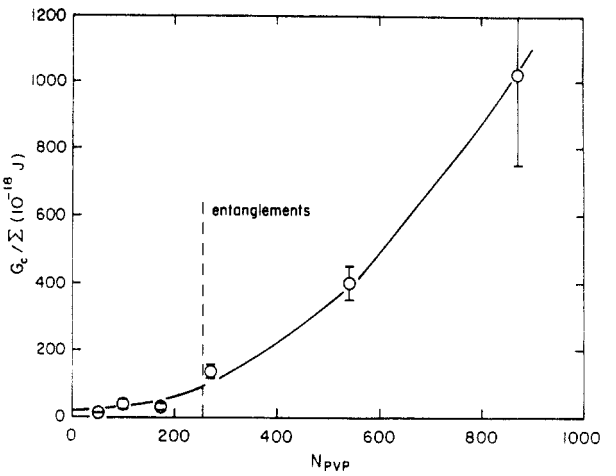

Figure 8. Fracture toughness per chain as a function of the degree of polymerization of the PVP block. The full line is to guide the eye.

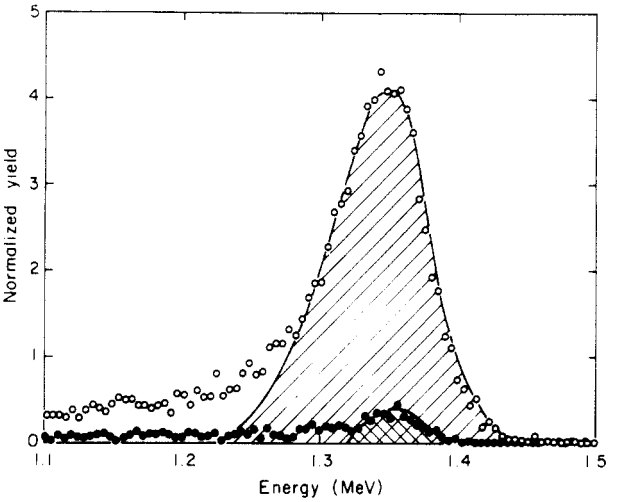

Figure 9. FRES spectra of the fracture surfaces of a sample reinforced with 0.058 chains/nm^2 of 1300–173 block copolymer: (○) deuterium on the PS side corresponding to 0.055 chains/nm^2; (●) deuterium on the PVP side corresponding to 0.003 chains/nm^2. The shaded areas are the amounts of deuterium used to determine Σ.

in Figure 10a, where the amount of iodine detected corresponds to about two-thirds of the PVP blocks of the copolymer chains being pulled out from the PVP side.

For the same 1300–173 copolymer, the surface composition obtained from XPS was found to correspond exactly to the amount of PVP which would be expected from a randomly organized layer of pure block copolymer at the surface. For the 280–52 and the 680–100 copolymers, the measurement of the surface composition indicated 4% and 4.5% of nitrogen on the surface, respectively. Such an amount is more than that which would be detected for a randomly organized layer of pure block copolymer, indicating an excess of PVP in the near-surface region (50 Å). This result is illustrated in Figure 10b with a plot showing the C 1s peak and the N 1s peak for the 680–100 polymer. The integrated area under the peaks, after normalization by the respective photoelectric cross-sections, is directly representative of the relative amounts of the elements present at the surface. The chemical shift in the peaks is due to the charging of the nonconductive sample. Although, strictly speaking, an accurate quantitative analysis cannot be done from the XPS results without a knowledge of the nitrogen concentration profile in the first 50 Å, these results combined with the RBS and the FRES results provide very strong evidence that the

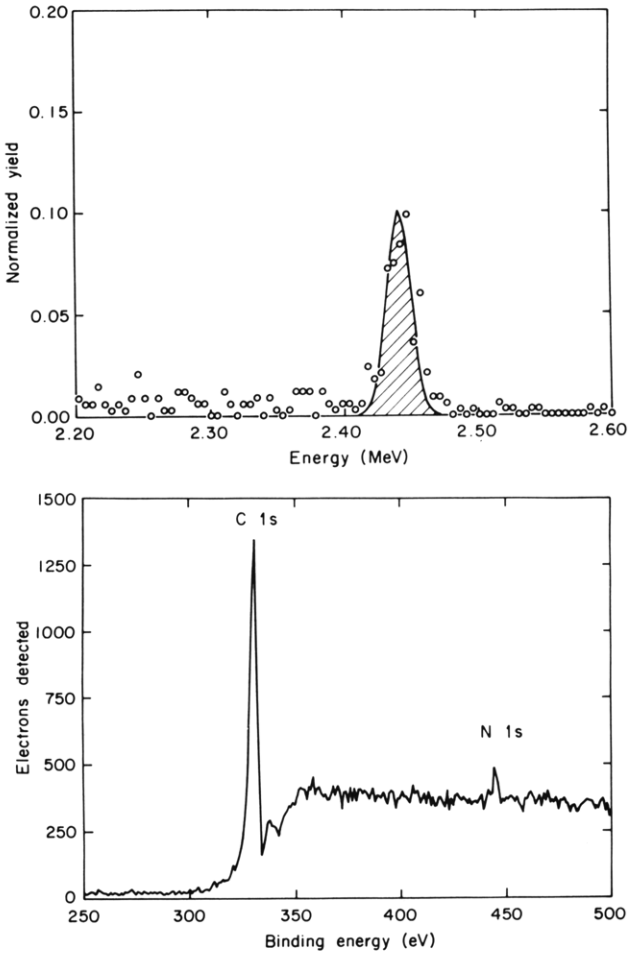

Figure 10. (a) RBS spectrum of the PS side of a sample with 0.058 chains/nm^2 of 1300–173 stained with methyl iodide. (b) XPS spectrum of the PS side of a sample with 0.02 chains/nm^2 of 680–100. The relative areas of the carbon and nitrogen peaks shown in the plot are indicative of the surface composition of the sample.

block copolymer chains do indeed pull out from the PVP side when $N_{PVP} < N_{ePVP}$.

4.4. Long PVP Block (N_{PVP} above N_{ePVP}). In this case, the results of the surface analysis are dependent not only on N_{PVP} but also on Σ, the areal density of block copolymers at the interface. For the 800–870 block copolymer almost all the deuterium is found on the PS side up to a total areal density of chains of 0.03 chains/nm^2 at which point a transition occurs and nearly all the deuterium is found on the PVP side as summarized in Figure 11. A similar transition, although shifted toward lower values of Σ, is observed for the 510–540 copolymer as well. This observed transition suggests that the locus of fracture changes from the area of the interface to the area of the brush between the dPS block and the PS homopolymer when Σ is increased above a certain critical value. A confirmation of this transition is given by the XPS data on the fracture surfaces. For the interface with 0.02 chains/nm^2 of 800–870 (below the transition) the surface composition shows that a small amount of nitrogen is present on the PS surface (about half the amount expected from a randomly organized layer of pure 800–870 block copolymer at the surface). On the other hand, for the interface with 0.05 chains/nm^2 of 510–540 copolymer (above the transition) there was no trace of nitrogen on the surface, confirming our hypothesis of breakdown in the brush between the PS and the dPS block.

This change in the locus of fracture as well as a large increase in the measured G_c above the transition suggests

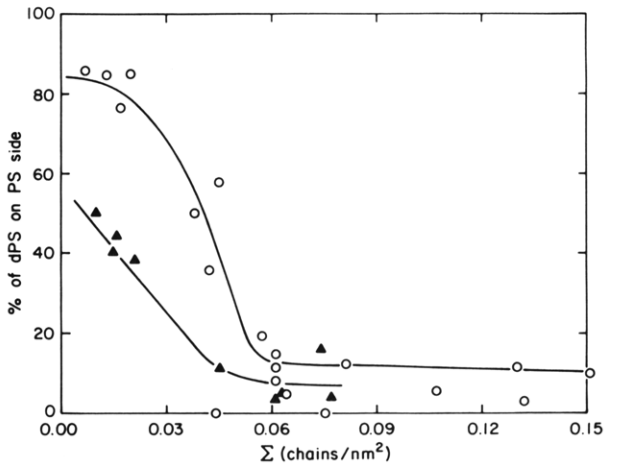

Figure 11. Percentage of dPS found on the PS side after fracture as a function of the areal density of chains at the interface: (○) 800–870 copolymer; (▲) 510–540 copolymer.

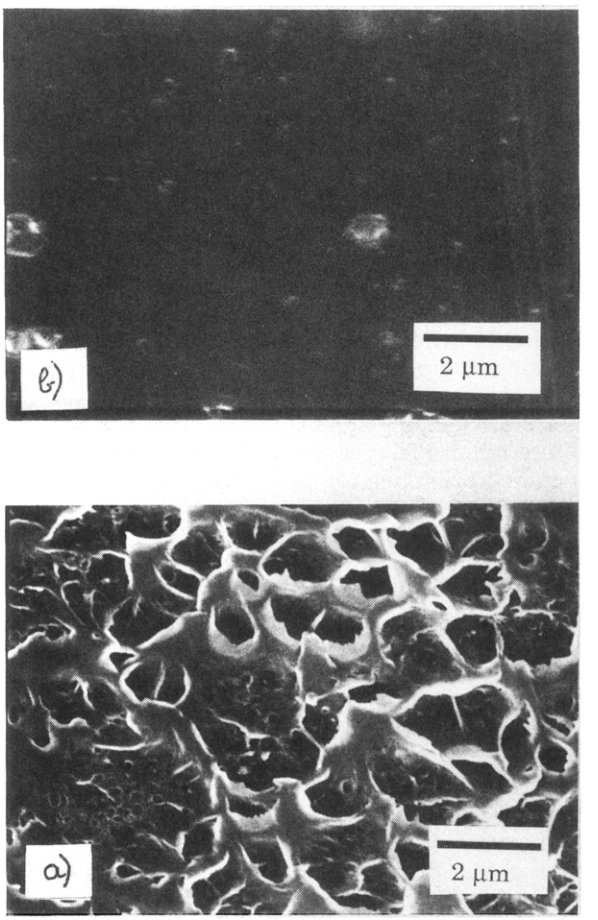

Figure 12. Scanning electron micrographs of the PVP surfaces after fracture of a sample reinforced with (a) 0.07 chains/nm^2 of 800–870 copolymer and (b) 0.015 chains/nm^2 of 800–870 copolymer.

a change in fracture mechanism with increasing Σ. More evidence supporting this assumption is given by the observation of the fracture surfaces by scanning electron microscopy. The difference in the appearance of the PVP fracture surfaces (above and below the transition) is very striking. While the fracture surface of a sample with 0.07 chains/nm^2 shown in Figure 12a shows clearly that gross plastic deformation must have taken place during the fracture process, the fracture surface of a sample with 0.015 chains/nm^2 in Figure 12b shows very little evidence of any plastic deformation occurring before fracture.

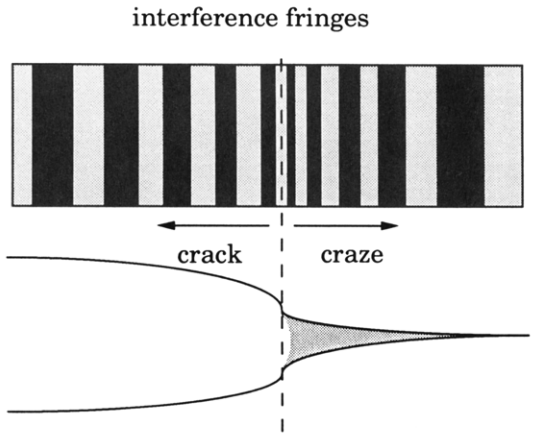

Figure 13. Schematics of the interference fringes obtained by reflected light microscopy off the crack faces and off the craze–bulk interfaces of a sample.

As both PS and PVP deform by crazing, it is reasonable to assume that crazing is the deformation mechanism responsible for the observed plastic deformation and the increase in G_c.

Direct evidence for the existence of a craze ahead of the crack tip can be obtained by optical interference microscopy. When a beam of monochromatic light is sent in a direction normal to the plane of the crack, it will reflect off both crack faces due to the index of refraction difference at the craze–bulk or at the crack–bulk interfaces. These two reflected beams will form interference fringes from which the thickness of the opening can be calculated provided the order of the fringe and the respective indices of refraction are known.[18] As shown schematically in Figure 13, the shape of the crack opening and the shape of the craze opening are different so that the spacing of the interference fringes always becomes smaller toward the crack tip, making it possible to determine unambiguously the presence of a craze ahead of the propagating crack. Interference fringes from a craze propagating at an interface reinforced with 0.07 chains/nm^2 of 800–870 block copolymer are shown in Figure 14a. The measured fracture toughness of that interface was approximately 70 J/m^2. When smaller amounts of block copolymer are added however, it is no longer possible to observe a craze at the crack tip as the resolution of the optical technique is limited to crazes with thicknesses larger than the wavelength of the incident light, i.e., 550 nm. The type of interference fringes obtained from a weak interface are shown in Figure 14b, and they are indistinguishable from the fringe pattern one would observe from a crack.

As a check of the validity of our measurement, it is worthwhile to compare the value of G_c that can be extracted from this direct measurement of the width of the craze with the G_c value obtained from the double cantilever beam test. The width of the craze h is given by

$$h = \frac{\lambda_0}{2\mu} n \tag{8}$$

where λ_0 is the wavelength of the incident light, μ is the index of refraction of the craze, and n is the order of the fringe. G_c is given by

$$G_c = h(1 - 1/\lambda)\sigma_d \tag{9}$$

where λ is the craze fibril extension ratio. With $n = 6$ from Figure 14a, $\lambda_0 = 550$ nm, $\mu \sim 1.15$,[19] $\lambda = 4$, and $\sigma_d = 55$ MPa, one obtains $G_c \sim 60$ J/m^2, in reasonable agreement with the value of 70 J/m^2 measured with the double cantilever beam test.

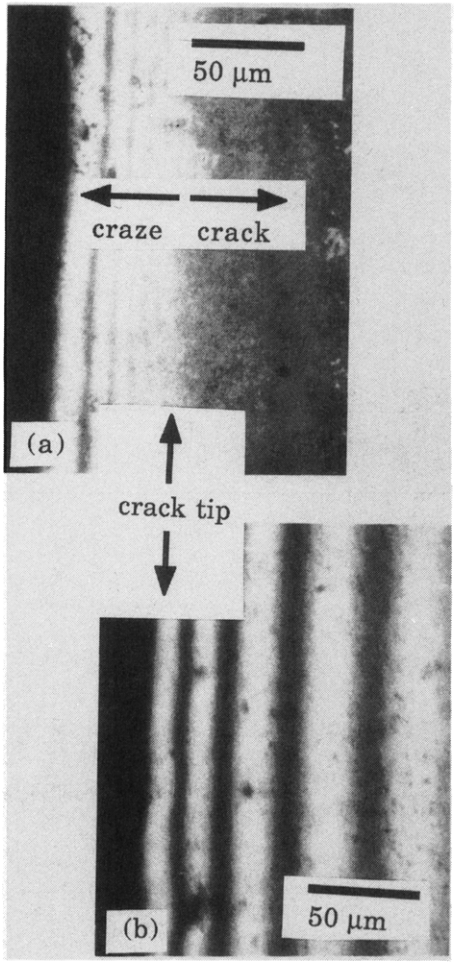

Figure 14. Interference fringes observed from reflected light microscopy: (a) interface reinforced with 0.07 chains/nm^2; (b) interface reinforced with 0.015 chains/nm^2.

5. Discussion

From the results presented in section 4, a simple model of the fracture mechanisms as a function of the two important variables, N_{PVP} and Σ, can be proposed. While the actual situation is somewhat more complicated than this simple model would allow, as we shall demonstrate, the model provides a very useful framework on which to understand the basic experimental observations.

For $N_{PVP} < N_{ePVP}$, the interface is very weak and the chains are pulled out from the PVP side so that the only energy-consuming mechanism is the friction energy from the viscous pull-out of the PVP block. When N_{PVP} becomes larger than N_{ePVP}, fracture occurs by chain scission rather than chain disentanglement. At low Σ, fracture occurs without any significant amount of plastic deformation and the chains break close to their midpoint, while at high Σ, it occurs by formation of a craze, the fibrils of which subsequently fail by chain scission in the region of the brush between the PS and the dPS block.

Although this picture is correct to a first approximation, it is interesting to examine it in more detail to point out its shortcomings. Furthermore, a more quantitative analysis of the experimental data can be done in view of some recently proposed models.

Following the idea that for chains with "short" PVP blocks failure occurs by PVP chain pull-out, Xu et al.[1] developed a model which assumes a brush of block copolymer chains at the interface as shown in Figure 15 and considers one-sided chain pull-out (i.e., only the PVP block pulls out from the PVP side; the PS block stays

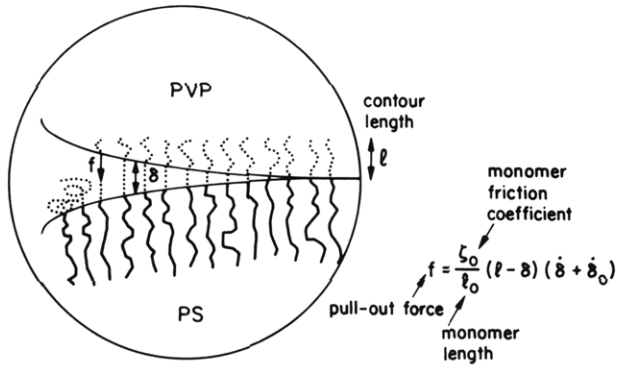

Figure 15. Schematic diagram showing the molecular picture described by Xu et al. in their chain pull-out model. The PS chain stays anchored to the bulk polymer while the shorter PVP chain is being pulled out by a viscous force.

anchored) as the only energy-consuming mechanism. This model provides some valuable physical insight. In particular, for the case of slow crack velocity ($\dot{a} \to 0$), G_c is given by

$$G_c = {}^1/_2\sigma_0 l \tag{10}$$

where l is the chain contour length (proportional to N_{PVP}) and σ_0 is a yield stress given by

$$\sigma_0 = \Sigma\zeta\dot{\delta}_0 l \tag{11}$$

where ζ is a friction coefficient and $\dot{\delta}_0$ is a proportionality constant which has units of velocity. Because the friction terms are not known a priori and are difficult to estimate, quantitative predictions cannot easily be made from this expression. It gives however a scaling prediction for the dependence on the areal density of chains and on the chain contour length which can be tested experimentally:

$$G_c \propto \Sigma l^2 \propto \Sigma N_{PVP}{}^2 \tag{12}$$

We measured G_c for several block copolymers with $N_{PVP} < N_{ePVP}$, and a linear dependence of G_c vs Σ was observed in all cases as shown in Figure 6. For two of the block copolymers, 1300–173 and 680–100, we observed a saturation plateau around $\Sigma_{sat} = 0.1$ chains/nm^2. In the case of 1300–173 this value of Σ_{sat} corresponds closely to the equilibrium amount of block copolymer segregated at the interface at $\mu = \mu_{cmc}$ as measured by FRES in a separate study.[17] Although there is no reason to believe that both saturations should occur for exactly the same areal density of chains, it is reassuring to see that the maximum reinforcement effect occurs for a thickness of block copolymer corresponding roughly to a saturated brush at the interface. Although at this point we do not have enough evidence to substantiate this claim, Σ_{sat} should be mostly controlled by the degree of polymerization of the longer block from simple space-filling arguments.

The dependence of G_c on the contour length of the chain being pulled out can be verified by plotting G_c/Σ vs N_{PVP} in a log–log plot. As shown in Figure 16, although G_c/Σ obviously increases with N_{PVP}, the agreement with the model is not very good. The main reason for this discrepancy lies probably in the poorly known conformation of the chains at the interface, which is influenced by the molecular weight of the longer PS block. For the two copolymers with a nearly equivalent PS block, i.e., 625–49 and 680–100, G_c/Σ scales reasonably well with l^2.

An important limitation of this pull-out model lies in the possibility of the existence of a craze ahead of the crack tip. Within the framework of Xu's model, the maximum stress that can be sustained by the interface is

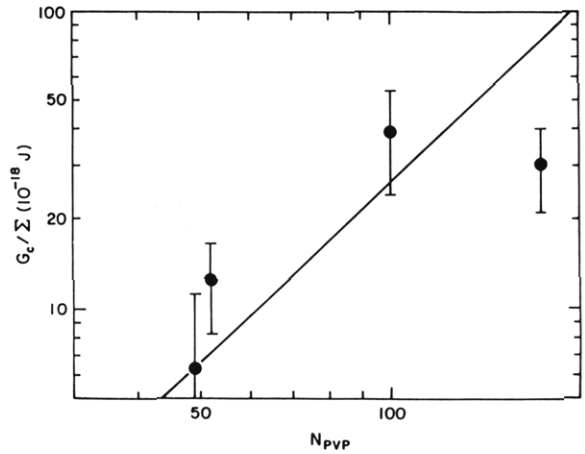

Figure 16. Fracture toughness per chain necessary to fracture the interface for the case of $N_{PVP} < N_{ePVP}$. The line is the best fit for a dependence of the type $G_c/\Sigma \propto N_{PVP}{}^2$.

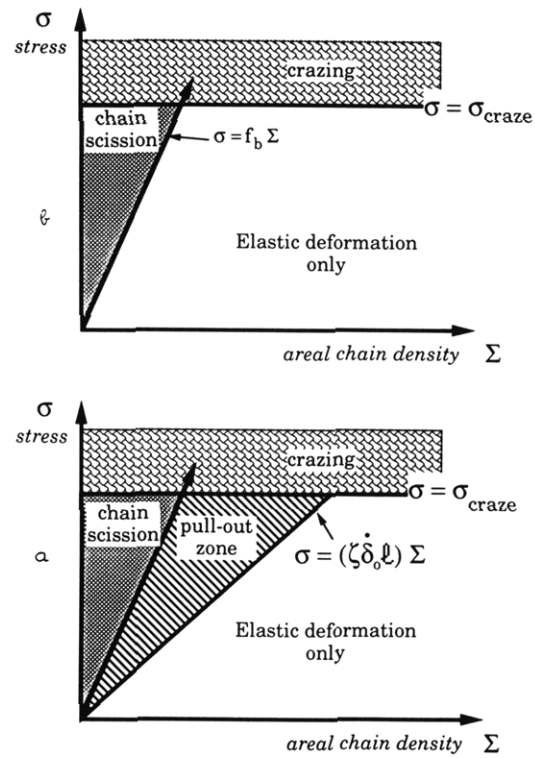

Figure 17. Schematic diagram of the stress at the interface as a function of the areal density of copolymer chains in the case where (a) chain pull-out is the dominant failure mechanism and (b) chain fracture is the dominant failure mechanism.

proportional to the areal density of chains at the interface as shown in Figure 17a. When the applied stress reaches the level of the crazing stress, there should be a transition in fracture mechanism from simple chain pull-out to crazing followed by chain pull-out. This transition allows us to make an upper bound prediction for G_c from eq 10 as σ_0 cannot be larger than σ_d, the craze-widening stress of the homopolymer.

In our specific case the homopolymer with the lower crazing stress is the PS so that it is reasonable to assume that the stress at the interface is bounded by the crazing stress of PS. With $\sigma_d = 55$ MPa as given by Table II and $l = 46$ nm characteristic of a chain with $N = 200 \sim N_e$, $G_c{}^{upper}$ can be estimated at 1.3 J/m^2. This value is still too low to account for our experimental results and suggests that other energy-consuming deformation mechanisms are active during fracture.

Recent transmission electron microscopy observations of microtomed thin films containing a single PS–PVP interface reinforced with 1300–173 block copolymer[20] have shown evidence of the presence of a very narrow craze at the crack tip, the thickness of which was consistent with the measured fracture toughness. Therefore it is possible that for larger Σ's the interface actually fails by first forming a narrow craze, the fibrils of which eventually fail by a disentanglement process in which the short PVP block pulls out.

Finally, it should be pointed out that the incorporation of a craze in the modeling of the fracture process as described in section 1.4, although increasing considerably the absolute values of the predicted G_c, does not change the scaling prediction given by Xu's model.

When $N_{PVP} > N_{ePVP}$, one expects the block copolymer chains to be effectively entangled with the PVP homopolymer so that the slope of the curve in Figure 17a becomes larger than the slope of the fracture curve given by

$$\sigma_{max} = f_b \Sigma_{eff} \tag{13}$$

with f_b being the force necessary to break a single polymer chain. As illustrated in Figure 17b, when the maximum stress that can be supported by the interface becomes larger than the crazing stress σ_d, the failure mechanism should undergo a transition from simple chain fracture involving very little plastic deformation to crazing. In principle, an estimate of the force to break a single polymer chain f_b can be extracted from eq 13 if the value of Σ at the transition is known.

A second transition deserves some attention and it is the change in the locus of fracture from the block copolymer midpoint to the brush between the PS and the dPS block. This experimental observation suggests that at high Σ the fracture takes place in the PS phase rather than exactly at the interface so that the craze formed might be mostly if not entirely in the PS phase. This hypothesis is based also on our measurements of the crazing stress showing that PS has a 30% lower crazing stress than PVP so that when the interfacial stress becomes higher than σ_d of the PS, a craze is nucleated at the interface and widens in the PS phase only. The craze will ultimately fail by fibril breakdown in the interfacial region, which remains the weakest point. This description has been confirmed by TEM observations of the crazing behavior of thin films containing a single interface between PS and PVP[20] showing that the craze widens exclusively in the PS phase and breaks at the craze–bulk interface, which coincides with the PS–PVP interface.

This second transition can be understood qualitatively by considering the concentration of non-load-bearing strands. For low Σ, the weakest part of the interfacial region is the interface itself, which contains an excess of chain ends from the homopolymers. When Σ increases, the block copolymer chains become more and more stretched so that a higher concentration of non-load-bearing strands is found in the region of the interface between the PS and the dPS block and fracture, presumably by chain scission, occurs then in the brush region.

As a first approximation it is tempting to postulate that both transitions should occur at the same point. Taking $\Sigma_{trans} = 0.03$ chains/nm^2 for the 800–870 copolymer as obtained from the surface analysis data in Figure 11 and 55 MPa for the PS crazing stress, one obtains from eq 13 $f_b = 1.8 \times 10^{-9}$ N, which is in good agreement with previously reported results.[2,21]

Unfortunately, there is some evidence that such an approach may not be accurate. The crazing transition should be only dependent on the chain scission force, while experimentally the brush transition occurs at different values of Σ for the 510–540 and 800–870 copolymers, namely, 0.01 and 0.03 chains/nm^2. More disturbing is the fact that crazes have been observed by TEM in single interfaces between PS and PVP[20] at values of Σ much below the brush transition. These experimental observations stress the difficulty of ascertaining unequivocally the existence of a craze at the crack tip, precluding us from giving an accurate value for f_b through this approach.

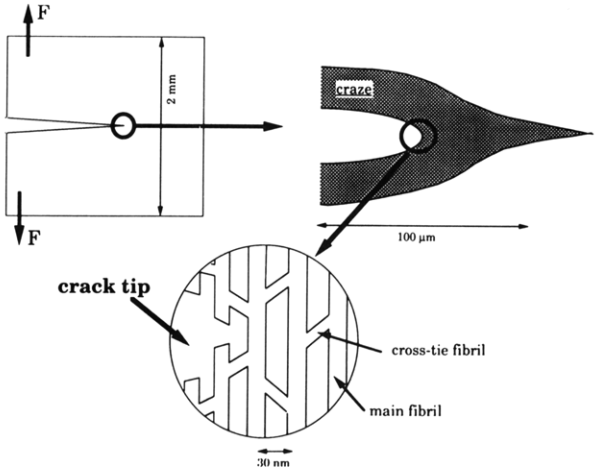

Figure 18. Schematic diagram showing a craze at the tip of a propagating crack. The craze is represented with cross-tie fibrils as described by Brown's model.

At values of Σ above this transition it is reasonable to assume that the propagating crack is preceded by a craze as described schematically in Figure 18. As a further indication of a change in fracture mechanism, the functional dependence of G_c is much less clear-cut than for the sub-M_e case: while at low values of Σ, G_c appears to increase as Σ^2, at higher values it clearly has a linear dependence.

These results can be analyzed in light of a model for craze breakdown proposed recently by Brown[2] and further extended by Hui et al.[22] which takes into account the existence of cross-tie fibrils in the fibril network of the craze. These cross-tie fibrils allow stress to be transferred from one main fibril to its neighbor so that the portion of the craze behind the crack tip is not completely unloaded after fracture and transfers an additional amount of stress to the last unbroken fibril, causing it to fail.

From this model, the critical energy release rate should scale as the square of the effective density of load-bearing strands present at the interface Σ according to the following expression (taken from Hui[22]):

$$G_c = \left(\frac{1}{A_c^2}\right)\frac{\Sigma^2 f_b^2 (2\pi D)}{\sigma_d}\left(\frac{S_{22}}{S_{12}}\right)^{1/2}(1 - 1/\lambda) \tag{14}$$

where A_c is a constant, D is the fibril diameter, λ is the craze fibril extension ratio, and S_{12} and S_{22} are the shear modulus and the tensile modulus of the fibrillar material, respectively.

When analyzing his data on interfaces between PMMA and PPO reinforced with PS–PMMA block copolymers, Brown implicitly assumed that this effective density of strands at the interface was equal to the areal density of block copolymers and found good agreement between his data and the proposed model.[2] In our system however such an approach would not give a very good agreement with the experimental data as evidenced by Figure 19.

This discrepancy can be understood in terms of the chain distribution at the interface by introducing the notion of

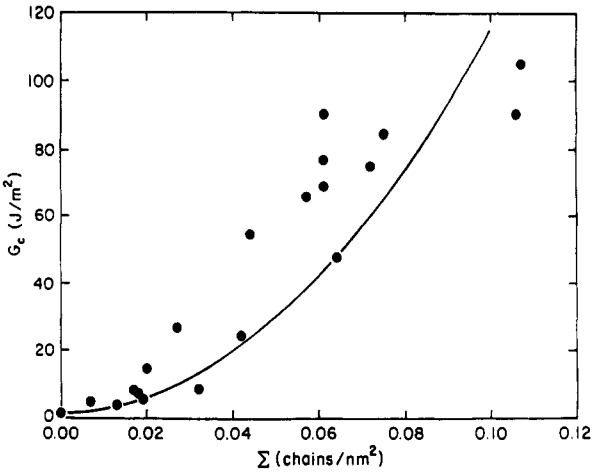

Figure 19. Fracture toughness G_c as a function of the areal density of block copolymer chains for the 800–870 copolymer: (●) data points; (—) best square fit.

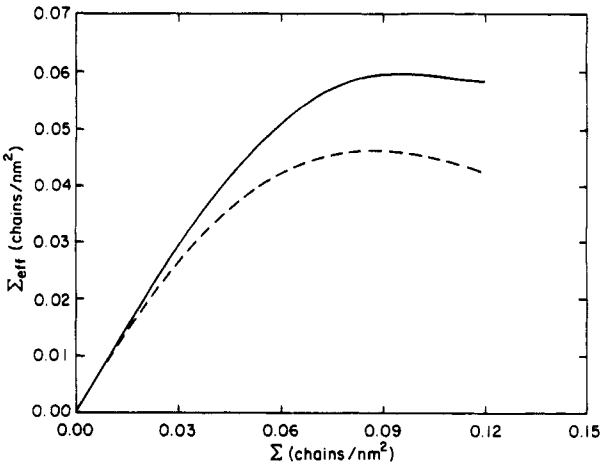

Figure 20. Areal density of chains with at least one effective entanglement (Σ_{eff}) as a function of the nominal areal density of chains (Σ): (—) 800–870; (- - -) 510–540.

effective entanglement. The assumption made here is that a given block of a block copolymer chain will have a reinforcing effect only if it has at least one effective entanglement with the homopolymer, where effective entanglement refers to an entanglement at least one N_e removed from the chain end of the respective polymers. Qualitatively, when the areal density of chains is increased, the block copolymer is more likely to be entangled with itself than with a homopolymer chain, therefore reducing the number of chains with at least one effective entanglement.

A more quantitative analysis of the distribution of effective entanglements can be done using the self-consistent mean-field theory developed by Shull and Kramer[23] for the study of block copolymer segregation at the interface. This method allows the calculation of the segment distribution function of the two homopolymers and of the block copolymer in the region near the interface by solving numerically a modified diffusion equation. Information on the number of effective entanglements between block copolymer chains and homopolymer chains can be extracted from the segment distribution function of the different components by making appropriate assumptions.

The detailed procedure given in Appendix A assumes that the probability of an effective entanglement between block A and homopolymer A is proportional to the probability of a contact between a segment of block A located at least one N_{eA} away from the chain end and a segment of homopolymer A located at least one N_{eA} away from the homopolymer chain end.

The average number of effective entanglements per chain $\bar{N}_{eff}$ is given as

$$\bar{N}_{eff} = \frac{\rho}{\Sigma N_{ea}(1 - 2N_{ea}/N_{ha})}\xi^* \qquad (15)$$

where ρ is the density of segments, N_{ha} and N_{ea} are the degrees of polymerization of homopolymer A and the average degree of polymerization between entanglements for polymer A, respectively, and ξ^* is a quantity obtained from the self-consistent mean-field simulation.

As a first approximation one can argue that when $\bar{N}_{eff} < 1$ there should be no further improvement in mechanical strength. However, a more relevant quantity is the areal density of chains with at least one effective entanglement Σ_{eff}. To obtain that quantity we need information on the distribution of entanglements in addition to their average number per chain.

This distribution can be found by using the same method and simply substituting the integration limits in eq A6 with the appropriate values to calculate the average number of effective entanglements of each portion of block copolymer of length N_e. Assuming that each entanglement is an independent event, i.e., that the probability of a chain to have an entanglement in its second portion does not depend on the occurrence of an entanglement in the first portion but only on the number of copolymer–homopolymer contacts, one can obtain a distribution of the number of entanglements per chain and therefore Σ_{eff}.

It should be pointed out also that a certain number of effective strands will be lost during the fibrillation process so that the actual areal density of effective strands reinforcing the interface will be even smaller than Σ_{eff}. Although in our case the actual entanglement loss will be dependent on the areal density of copolymer chains at the interface, a quantitative estimate of this necessary entanglement loss as previously derived for random coils[24] can be used for the purpose of quantitative comparison with experimental data. For PS, Σ'_{eff} will then be given by

$$\Sigma'_{eff} = q\sigma_{eff} = 0.6\Sigma_{eff} \qquad (16)$$

where q is the surviving fraction of load-bearing strands after fibrillation. This additional factor will only be important when quantitative predictions are made and, in particular, to obtain the force to break a single strand f_b from eq 14. For the sake of comparing our results with Brown's[2] we deliberately ignored this additional multiplication constant in the plots of G_c vs Σ given in Figures 21 and 22.

To illustrate the main result of our calculation, a plot of Σ_{eff} vs Σ is shown in Figure 20 for the 800–870 polymer and the 510–540 polymer. From the surface analysis results it is clear that at high Σ, the craze ultimately fails in the region of the brush between the dPS block and the PS homopolymer. Σ_{eff} refers therefore to the areal density of dPS blocks with at least one effective entanglement. For the mean-field simulation we used $\chi_{PS\text{-}PVP} = 0.11$, $N_{ePS} = 173$, and the degree of polymerization of the homopolymers $N_{hPS} = N_{hPVP} = 2150$. While Σ_{eff} increases linearly with Σ at low copolymer densities, it rapidly deviates from linearity, reaches a maximum, and finally slightly decreases. It should be pointed out that for blends the maximum copolymer excess that can be present at the interface is controlled by the chemical potential of the free copolymer chains in the bulk μ_c; hence, when $\mu_c = \mu_{cmc}$, no further segregation can occur. For these two

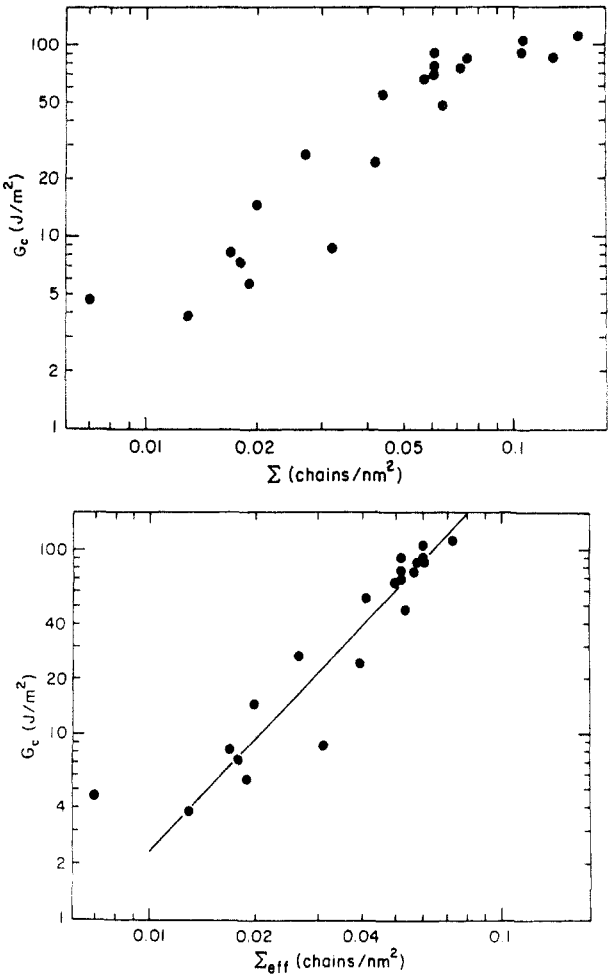

Figure 21. Fracture toughness G_c for the 800–870 copolymer as a function of (a) the nominal areal density Σ of copolymer chains and (b) the areal density Σ_{eff} of copolymer chains with at least one effective entanglement.

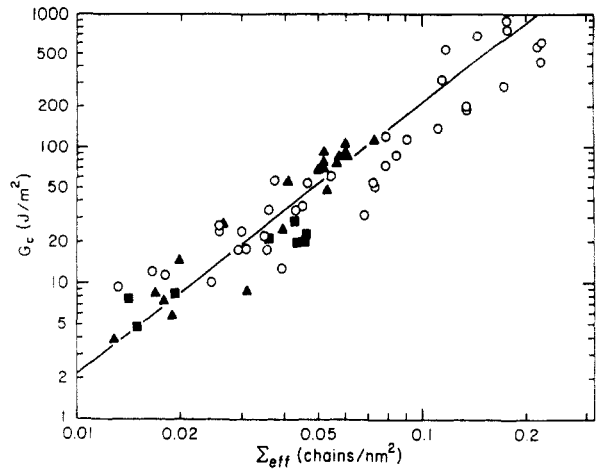

Figure 22. Fracture toughness of interfaces reinforced with block copolymer as a function of the effective areal density of chains Σ_{eff}: (▲,■) PS–PVP data from this study; (○) PS–PMMA data from Brown;[2] (—) best square fit.

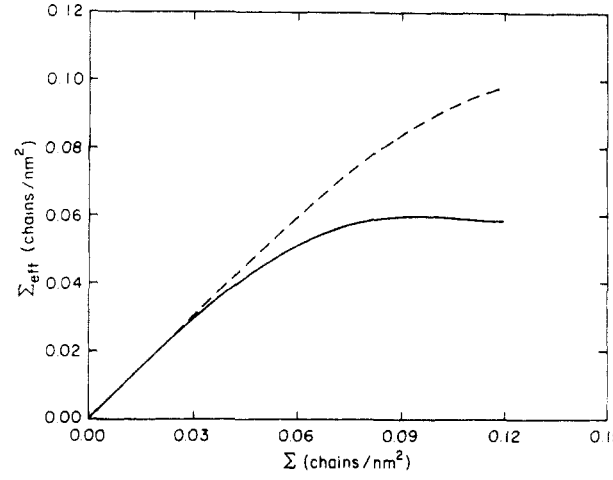

Figure 23. Effective areal density of copolymer chains as a function of nominal areal density for an 800–870 copolymer with (—) N_{ePS} = 173 and (– – –) N_{ePS} = 90.

polymers an estimate of μ_{cmc} can be obtained from the expression given in ref 16, and the corresponding maximum amount of chains present at the interface is 0.091 and 0.102 chains/nm^2 for the 800–870 and 510–540 copolymers, respectively. However, in our experiments, the amount of copolymer present at the interface can be higher as the very slow kinetics prevent the excess copolymer from being drained away effectively from the interface.

For the 800–870 block copolymer, the logarithm of the fracture toughness of the interface G_c is plotted vs log (Σ) in Figure 21a and vs log (Σ_{eff}) in Figure 21b. It is very clear from the plots that the data fit a power law much better when they are plotted vs Σ_{eff}. The slope of the linear fit gives $G_c \propto (\Sigma_{eff})^{2.02}$, consistent with Brown's model of craze breakdown.

According to eq 14 the fracture toughness should only depend on the crazing stress σ_d, the craze fibril extension ratio λ, and the areal density of strands Σ so that data for different block copolymers should fall on the same master curve if they are plotted as $(G_c\sigma_d)/(1 - 1/\lambda)$ vs Σ. In principle, the chain breakage force f_b should be independent of the chemical features of the polymer provided the backbone is composed of carbon–carbon bonds only, while the fibril diameter D is similar for PS and PMMA.

Our data on the 800–870 and 510–540 copolymers are compared in Figure 22 with Brown's data on PMMA–PPO interfaces reinforced with PS–PMMA block copolymers of various molecular weights, where Brown's data have been multiplied by $[\sigma_d(PMMA)/\sigma_d(PS)]$ and corrected for the different values of λ_{PS} and λ_{PMMA}. The value of the crazing stress for PMMA is taken as 100 MPa as measured by the three-point bending test. It is reassuring to see that the two sets of data fall nearly on the same line and follow fairly well a constitutive law of the type $G_c \propto \Sigma_{eff}^2$, providing a confirmation of the validity of the model. Another check can be obtained by calculating the force to break a single chain from eq 14. By using D = 10 nm, σ_d(PS) = 55 MPa, λ_{PS} = 4, A_c = 0.794, and S_{22}/S_{12} = 55–130 from ref 22 and taking into account the necessary loss of entanglements due to the fibrillation process, one obtains $f_b \sim (3.5 \pm 0.5) \times 10^{-9}$ N, which is a reasonable result consistent with previously reported values.[2,21]

It should be noted that Brown's data are plotted vs Σ rather than Σ_{eff} and follow nevertheless a square law. A possible explanation could lie in the difference in N_e between PS and PMMA. As PMMA has a lower crazing stress than PPO, it is likely that the interface fails by forming a craze in the PMMA phase. A lower N_e will allow more entanglements per chain, therefore shifting the maximum predicted in the Σ_{eff} vs Σ plot in Figure 20 toward higher values of Σ. To substantiate this hypothesis we repeated the calculation of Σ_{eff} for the 800–870 block copolymer, assuming this time that N_e was only 90 rather than 173. The results of this calculation are shown in Figure 23 and indeed confirm the validity of our interpretation.

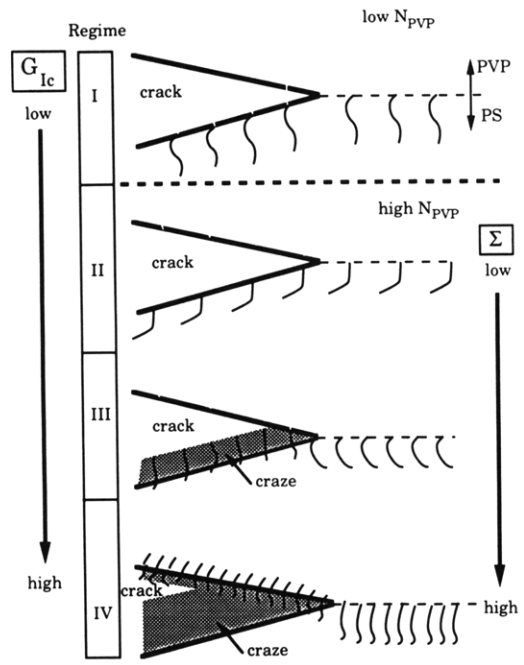

Figure 24. Schematic diagram of the four deformation regimes occurring in the fracture of interfaces between PS and PVP reinforced with PS–PVP block copolymers.

Concerning the fracture mechanism, the analysis of the fracture surfaces with secondary ion mass spectrometry (SIMS) showed that the block copolymer chains fractured very close to their midpoint.[25] The sample analyzed by Brown had an areal density of chains of $\Sigma = 0.05$ so that his result is reasonably consistent with our observations on the locus of fracture at low Σ.

6. Conclusions

The addition of PS–PVP block copolymers to interfaces between immiscible homopolymers PS and PVP always causes a reinforcement of the interface characterized by an increase in G_c. The effectiveness of the reinforcement and the nature of the failure mechanisms at the interface are however strongly dependent on the respective molecular weights of the blocks and on the areal density of chains at the interface. Four main regimes can be distinguished as summarized in Figure 24.

In the first regime (I) where $N_{PVP} < N_{ePVP}$, the chains are pulled out without any significant amount of plastic deformation; this is the case of the weakest interfaces. If Σ is increased above a certain critical level which probably depends on the length of the short block, the interface may actually fail by first forming a craze at the crack tip. This craze however is very unstable and will not grow in width more than 250 nm before failing by chain disentanglement of the shorter block.

When $N_{PVP} > N_{ePVP}$ three regimes are possible. In regime II at very low Σ, the interface fails without any significant amount of plastic deformation at the crack tip at a level of stress below the crazing stress σ_d. The block copolymer chains break very close to their midpoint, and the resulting values of G_c are low.

In regime III at slightly higher values of Σ, the stress at the interface is now high enough to form a craze. The interface now fails by the breakdown of the craze, the fibrils of which break by scission of the block copolymer chains close to the area of the joint between the two blocks.

When Σ is further increased, the region of the brush between the dPS block and the PS homopolymer becomes the weakest part of the interface and the fibrils of the propagating craze fail by chain scission in the brush region. In this regime, the craze preceding the crack can grow to a width up to several microns, causing measured values of G_c which come close to the fracture toughness of the homopolymers. It is clear from our results that those copolymers with the highest degrees of polymerization were the most effective mechanically. However, one expects that G_c/Σ vs N will level off at a certain value of N while the maximum areal density of chains with at least one effective entanglement Σ_{eff} will go through a maximum and then decrease for very large values of N, mirroring the decrease in the maximum attainable areal density of chains. More comprehensive calculations based on the self-consistent mean-field theory as well as new experimental results from copolymers with higher degrees of polymerization should result in a prediction of the most effective molecular weight for mechanical reinforcement.

One should bear in mind however that kinetic factors which dramatically increase equilibration times will be the limiting factor in the use of the most effective block copolymer so that a compromise between good mechanical performance and reasonable equilibration times is more likely to be necessary.

Acknowledgment. We gratefully acknowledge the support of this work by the NSF–DMR–MRL program through the Cornell Materials Science Center. We also appreciate the help of Fei Xiao for the fracture toughness experiment and Daben Xu in developing some of the models as well as the help of Elizabeth Carr for the XPS experiment. The block copolymers were synthesized with the help of Dr. Kenneth Shull, Kevin Dai, and Mildred Calistri-Yeh. Finally, we thank Dr. Jerry Seitz from Dow Chemical Co. for the plateau modulus measurements of PVP.

7. Appendix: Determination of the Effective Entanglement Density

In a ternary mixture of A, B, and C segments each occupying a site in a lattice, the fraction of the total contacts that are contacts between A and B segments is given by

$$\gamma_{A-B} = 2\phi_A\phi_B/z \tag{A1}$$

where ϕ_A and ϕ_B are the volume fractions of the A and B segments, respectively, and z is the coordination number of the lattice.

This result can be applied to our specific problem where the relevant volume fractions are now ϕ_{ca}^* and ϕ_{ha}^*, i.e., the volume fractions of "effective" segments for the A block of the copolymer (ca) and the homopolymer A (ha), respectively, an "effective" segment being defined as a segment at least N_e units away from a chain end.

The number of ha–ca contacts per unit area of interface is then given by

$$\xi_{ha-ca} = \frac{2\rho}{z}\int_{-\infty}^{+\infty} \phi_{ha}^*(x)\,\phi_{ca}^*(x)\,dx \tag{A2}$$

where ρ is the density of segments and x is the position relative to the interface. In the limit of $\phi_{ca} \to 0$, i.e., a vanishingly small volume fraction of copolymer, the areal density of effective entanglements ν_{eff} will be proportional to the areal density of copolymer chains or more exactly

$$\nu_{eff}(0) = (N_{ca}/N_{ea} - 1)\Sigma \tag{A3}$$

with N_{ca} and N_{ea} being the degree of polymerization of block A and the average degree of polymerization between entanglements for polymer A, respectively. Using the self-consistent mean-field theory, the segment distribution of

copolymer chains near the interface and subsequently the areal density of copolymer chains Σ can be evaluated:

$$\Sigma = \frac{\int_{+\infty}^{-\infty} \phi_{ca}\, dx}{N_{ca}}\rho \tag{A4}$$

It should be noted that although, strictly speaking, eq A4 is only valid if there is no amount of block copolymer dissolved in the bulk, in practice, the numerical integration is only carried out over a distance of ~1000 Å near the interface so that this expression is still valid as long as ϕ_c(bulk) is negligible. This condition is generally met for very incompatible systems and long copolymer chains.

The total number of effective entanglements per unit area is assumed to be proportional to the probability of a contact between an "effective" homopolymer segment and an "effective" copolymer segment. This probability is proportional to ξ^*, given by

$$\xi^* = \int_0^{\infty} \phi_{ca}^*(x)\, \phi_{ha}^*(x)\, dx \tag{A5}$$

with ϕ_{ca}^* and ϕ_{ha}^* as follows:

$$\phi_{ca}^* = A_{ca}\int_0^{(N_{ca}-N_{ea})/N_{ca}} q_{ca}(x,t)\, q_{ab}(x,1-t)\, dt \tag{A6}$$

$$\phi_{ha}^* = A_{ha}\int_{N_{ea}/N_{ha}}^{(N_{ha}-N_{ca})/N_{ha}} q_{ha}(x,t)\, q_{ha}(x,1-t)\, dt \tag{A7}$$

where q_{ha}, q_{ba}, and q_{ab} are distribution functions and A_{ca} and A_{ha} are proportionality constants as defined in ref 23. In the limit of $\phi_{ca} \to 0$, eq A5 becomes

$$\xi^*(0) = (1 - 2N_{ea}/N_{ha})(1 - N_{ea}/N_{ca})\int_{-\infty}^{+\infty} \phi_{ca}\, dx \tag{A8}$$

where the first term of eq A8 is the value of ϕ_{ha}^* when $\phi_{ca} \to 0$, while the second term is the normalization factor introduced by only considering segments that are N_{ea} away from the copolymer chain end.

The areal density of effective entanglements can be written as

$$\nu_{eff} = \xi^* K \tag{A9}$$

which reduces to eq A3 in the low copolymer density limit so that the proportionality constant K can be extracted as

$$K = \frac{\rho}{N_{ea}(1 - 2N_{ea}/N_{ha})} \tag{A10}$$

from which the areal density of entanglements at the interface can be obtained by substituting eq A10 into eq A9:

$$\nu_{eff} = \frac{\rho}{N_{ea}(1 - 2N_{ea}/N_{ha})}\xi^* \tag{A11}$$

ν_{eff} is the total number of effective entanglements per unit area. To obtain the areal density of chains with at least one effective entanglement (Σ_{eff}), some information on the distribution of entanglements in addition to their average number per chain is necessary.

This information can be obtained by using the method explained above and simply substituting the integration limits in eq A6 with the appropriate values to calculate the average number of effective entanglements of each portion of block copolymer of length N_e. Assuming that each entanglement is an independent event, i.e., that the probability of a chain to have an entanglement in its second portion does not depend on the occurrence of an entanglement in the first portion but only on the number of copolymer–homopolymer contacts, one can obtain the areal density of chains Σ_n with exactly n entanglements with the homopolymer. It is easy to see that Σ_{eff} is then

$$\Sigma_{eff} = \sum_{n=1}^{n_{max}} \Sigma_n = 1 - \Sigma_0 \tag{A12}$$

where n_{max} is the maximum number of effective entanglements per copolymer chain given by the integer part of N_{ca}/N_{ea} and Σ_0 is the areal density of chains with no entanglements.

References and Notes

(1) Xu, D.-B.; Hui, C.-Y.; Kramer, E. J.; Creton, C. *Mech. Mater.* **1991**, *11*, 257.
(2) Brown, H. R. *Macromolecules* **1991**, *24*, 2752.
(3) Fayt, R.; Jérôme, R.; Teyssié, P. *J. Polym. Sci., Polym. Phys. Ed.* **1982**, *20*, 2209.
(4) Fayt, R.; Jérôme, R.; Teyssié, P. *J. Polym. Sci., Polym. Chem. Ed.* **1989**, *27*, 2823.
(5) Lindsey, C. R.; Paul, D. R.; Barlow, J. W. *J. Appl. Polym. Sci.* **1981**, *26*, 1.
(6) Knaub, Ph.; Camberlin, Y.; Gérard, J.-F. *Polymer* **1988**, *29*, 1365.
(7) Creton, C.; Kramer, E. J.; Hadziioannou, G. *Macromolecules* **1991**, *24*, 1846.
(8) Brown, H. R.; Char, K.; Deline, V. R. *Integration of Fundamental Polymer Science and Technology*; Lemstra, P. J., Ed.; Elsevier: Amsterdam, 1991; Vol. 5.
(9) Brown, H. R. *J. Mater. Sci.* **1990**, *25*, 2791.
(10) Charalambides, P. G.; Cao, H. C.; Lund, J.; Evans, A. G. *Mech. Mater.* **1990**, *8*, 269.
(11) Bessonov, M. I.; Kuvshinskii, E. V. *Sov. Phys.*—Solid State (*Engl. Transl.*) **1959**, *1*, 1321.
(12) Kambour, R. P. *J. Polym. Sci., Part A-2* **1966**, *4*, 349.
(13) Tada, H. *The Stress Analysis of Cracks Handbook*; Del Research Co.: Hellertown, PA, 1973.
(14) Kanninen, M. F. *Int. J. Fract.* **1973**, *9*, 83.
(15) Seitz, J. Dow Chemical Co., private communication.
(16) Berger, L. L. Ph.D. Thesis, Cornell University, 1987.
(17) Shull, K. R.; Kramer, E. J.; Hadziioannou, G.; Tang, W. *Macromolecules* **1990**, *23*, 4780.
(18) Döll, W. *Adv. Polym. Sci.* **1983**, *52/53*, 105.
(19) Doyle, M. J. *J. Polym. Sci., Polym. Phys. Ed.* **1975**, *13*, 2429.
(20) Washiyama et al., to be published.
(21) Kausch, H. H. *Polymer Fracture*, 2nd ed.; Springer-Verlag: Berlin, 1987.
(22) Hui, C.-Y.; Ruina, A.; Kramer, E. J.; Creton, C., to be published.
(23) Shull, K. R.; Kramer, E. J. *Macromolecules* **1990**, *23*, 4769.
(24) Kramer, E. J.; Berger, L. L. *Adv. Polym. Sci.* **1990**, *91/92*, 1.
(25) Brown, H. R.; Deline, V. R.; Green, P. F. *Nature* **1989**, *341*, 221.